to force the polymer to swell in organic solvents, he and Inganäs investigated the behavior of PEDOT-PSS blends with PEO, which are known to form conductive PEDOT-PSS networks in a PEO matrix that could provide space for ionic movements.

Films of the polymer blends were cast onto gold-coated silicon wafers from aqueous dispersions and used as active electrodes. Cyclic voltammetry indicated that the PEDOT-PSS/PEO blends show the expected higher ionic mobility. Although the measured current is lower than for swollen hydrogels, the two values become comparable if they are normalized to the mass of PEDOT-PSS that is present in each electrode. This indicates similar efficiencies for both systems. The efficiency of the blend electrode increases with decreasing PEDOT-PSS content (down to about 25%), showing that the high compatibility of the two polymers allows the formation of a network morphology even at low PEDOT-PSS concentrations. Supercapacitor measurements gave high energy densities for the blend electrodes even at power densities five times higher than the drop-off for pure PEDOT-PSS electrodes. "These power densities were calculated using the total weight of the blend", Ghosh said. "This means that we get higher energies with a smaller amount of redox material."

"The increase in ionic mobility in the PEDOT-PSS blend with inclusion of PEO can be ascribed to the intrinsic ionic conductivity of the latter polymer as well as to the swelling of the PEO phase in the acetonitrile solution, creating space for ionic movement," Inganäs said. The researchers reported that the comparative experiments with blended and unblended PEDOT-PSS electrodes in a solid-state cell suggest that "the intrinsic ionic conductivity of PEO does contribute to the enhancement of ionic mobility."

Currently, the group is working "on better crosslinking of the electronically conducting PEDOT-PSS phase and on loading the material with more energy-rich material to increase the energy density, keeping the network morphology and hence the ionic mobility intact," said Ghosh. In the hydrogels, this has been achieved by introduction of polypyrrole, a second conducting polymer.

CORA LIND

Versatile Pattern Transfer Process for Polymers Developed

Researchers from the University of Massachusetts and the University of Groningen, The Netherlands, have reported a nanoscopic pattern transfer phenomenon. Erik Schaffer, a graduate student at Groningen, and Thomas Thurn-Albrecht, a postdoctoral researcher at Massachusetts, placed a thin film of polystyrene atop an electrode. They placed a second electrode above the film, leaving an air gap between the film and the top electrode. They then heated the polystyrene, liquefying it, and placed a small voltage on the electrodes.

With time, as reported in the February 24 issue of *Nature*, the surface of the film appeared pockmarked. Tom Russell, in polymer science and engineering at Massachusetts, said that the electric field amplified waves on the liquid's surface. The waves were increasingly amplified and eventually were pulled to the top electrode. The phenomenon appears under the microscope as a dark ring on a light background. As time passed, more and more circles appeared. The circles were all the same size, and appeared at a precise distance from one another.

Russell said that the phenomenon occurs because of the interaction of four competing forces. Those forces include the electrical force, which pulls the liquid toward the top electrode; the surface energy of the liquid, which wants the liquid to lie flat; the viscosity of the liquid as crests and valleys form and the liquid moves; and the effects of atmospheric pressure. "It doesn't happen helter-skelter," he said. "It happened at very distinct distances that represents a delicate balance between all of these forces."

Through a process called pattern transfer, the researchers can "imprint" a film with a very specific design. In this process, an electrode is etched with a master pattern. The master electrode has a topography of "hills" and "valleys." When a voltage is applied, the film responds most strongly to the closest portions of the electrode, creating a replica of the master design on the polymer film. The researchers said that their findings have implications in paving the way for still-smaller integrated circuits, magnetic storage in computers, and on-chip sensors—all of this without the use of chemicals.

Additional CeO_2 Buffer Layer Improves Performance of Superconducting Tape

The microstructural development of a superconducting tape (coated conductor) consisting of a layer of $YBa_2Cu_3O_y$ (Y-123) superconducting material (1–3-μm thick) on an Inconel 625 substrate 100-μm thick with a layer of yittria-stabilized zirconia (YSZ) 0.8-μm thick and CeO_2 buffer layers (~0.03-μm thick) was studied by researchers at the Los Alamos National Laboratory (LANL). They reported in the May 2000 issue of the *Journal of Materials Research* that an additional buffer layer is useful "for removing the misfit strain from the interface with the superconductor and limiting the extent of interfacial reactions with Y-123."

Since its discovery, Y-123 has been actively investigated for high critical current and high current density applications at liquid nitrogen temperatures. The epitaxially prepared materials studied at LANL exhibit the best critical current and current density in a 1 m Y-123 tape produced to date. These favorable characteristics are believed to result from the use of two buffer layers between the substrate and the superconducting film. The YSZ buffer layer improves performance by preventing the Ni and Cr from the substrate from contaminating the Y-123 layer and providing a biaxially aligned template for its growth. The CeO_2 buffer layer is believed to improve conductor performance by removing the lattice mismatch strain between the YSZ and Y-123 layers. To extend the current technology to the production of conductors longer than 1 m, and possibly improve conductor performance, the microstructural properties of the conductor during processing need to be investigated. This study detected and explained a number of such features.

A Cr_2O_3 layer was detected between the substrate and the YSZ layers by electron diffraction and energy dispersive spectroscopy. The researchers speculate that this layer formed *in situ* during the high temperature deposition of the CeO_2 and Y-123 layers and not during the room temperature deposition of the YSZ. The researchers believe that it is the Cr_2O_3 layer that prevents Ni and Cr from the Inconel from contaminating the Y-123, as neither metal could be detected above the Cr_2O_3. This is an important finding because it proves that the Inconel substrate is compatible with the YSZ layer. This is advantageous because YSZ is the only material known that can be reliably deposited as a biaxially textured film for Y-123 deposition.

No evidence for a reaction between YSZ and CeO_2 was detected; however, there was evidence of misfit dislocation between the layers. According to the researchers, since Y-123 is closely lattice matched to CeO_2, the extra buffer layer apparently moves the misfit strain away from the Y-123 film. The researchers reported, "A volume constraint imposed by the overlying Y-123 film may act as a kinetic barrier and limit the extent of the

https://doi.org/10.1557/mrs2000.64 Published online by Cambridge University Press

reaction." This result confirms the hypothesis that CeO_2 improves performance by removing the misfit strain between YSZ and Y-123.

The formation of several secondary phases was detected between CeO_2 and Y-123 indicating chemical reactions between the two layers. The formation of these phases is believed to have occurred after the deposition of the Y-123 because the biaxially textured structure of the Y-123 was not affected by the presence of a different phase below it. The reactions between these layers liberated material from the CeO_2 layer which diffused into the Y-123 layer as planar defects causing many gaps and cracks in this layer. These defects did not significantly affect the performance of the conductor used in this study but they may pose a problem for thicker layers of Y-123 or those deposited at higher temperatures.

GREGORY A. KHITROV

Development of Poly(ferrocenophane) Yields a Moldable Magnetic Ceramic Material

Researchers from the University of Toronto have reported in the February 25 issue of *Science* a step toward tunable, ceramic magnets. Mark J. MacLachlan and colleagues transformed iron-and-polymer molecules into a magnetic ceramic material, which was molded into various shapes. The key to the process is a technique for opening the rings in polymers. The group begins with monomers of silaferrocenophane (SFP). Subjecting the SFP to gentle heat produces poly(ferrocenylsilane), or PFS. Poured into molds of various shapes and subjected to more low heat, the molecules in this precursor material transform into a cross-linked network, which is loaded with trapped iron.

High doses of heat in a pyrolysis chamber sets the encapsulated iron free to seek other iron and form nanoclusters. Because larger clusters are more strongly magnetic, or ferromagnetic, the researchers can tune the material's magnetism by adjusting the temperature inside the pyrolysis chamber. Around 500°C, the structure transforms, and iron starts coming together. The size of the clusters grows in correlation with higher temperatures.

Molded into different shapes, such a material may be useful for high-density data storage, antistatic coatings for aircraft or spacecraft, among other applications, according to the research team. □

Correction

In *MRS Bulletin*, March 2000 issue, page 45, an incorrect illustration ran in Figure 11c from the article "Science and Applications of Mixed Conductors for Lithium Batteries," by Michael M. Thackeray, John O. Thomas, and M. Stanley Whittingham. See the corrected full figure that follows.

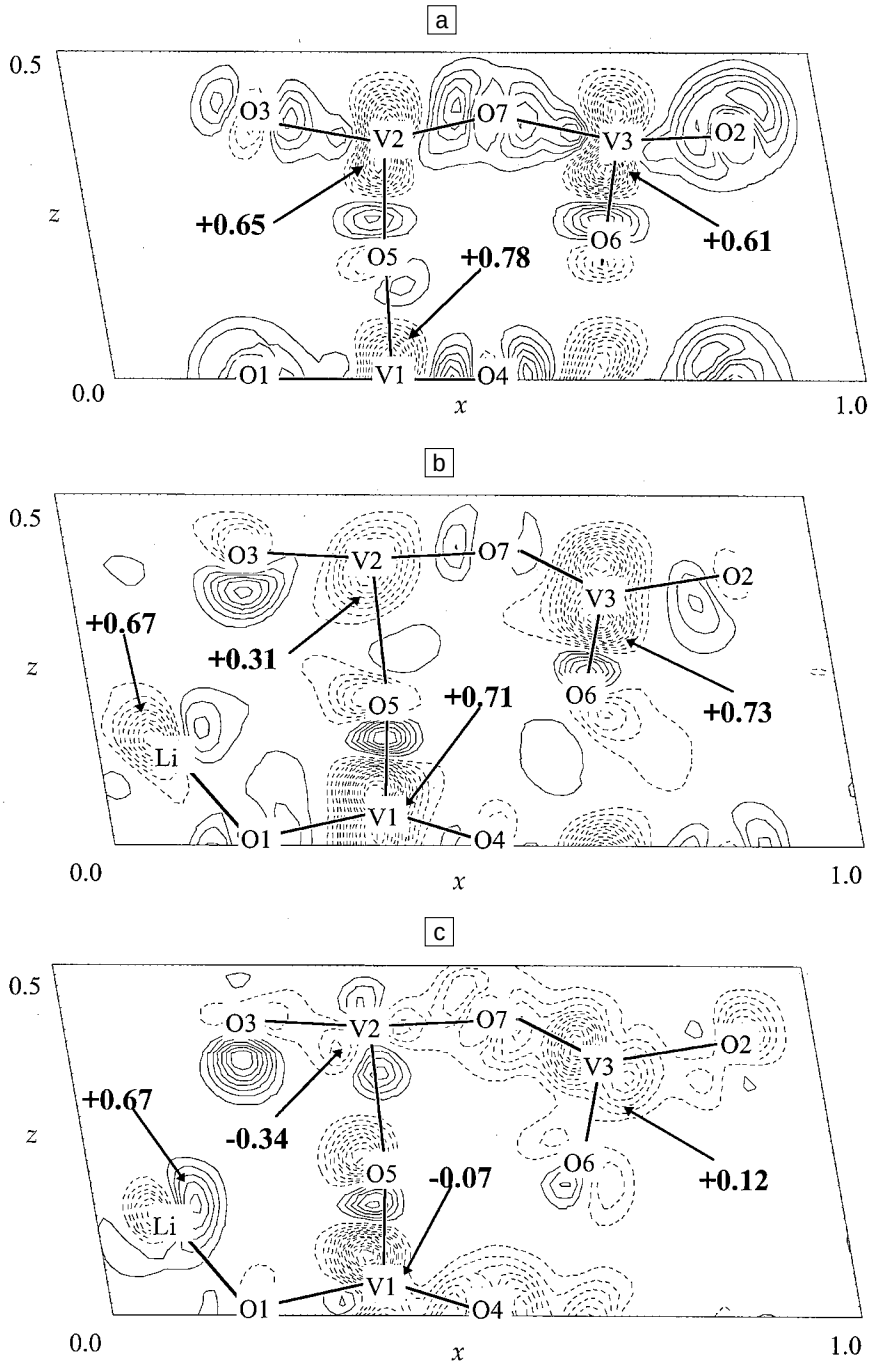

Figure 11. Deformation electron-density maps for (a) V_6O_{13} and (b) $Li_2V_6O_{13}$, and (c) the difference deformation electron-density map ("$Li_2V_6O_{13}$ -V_6O_{13}") in the a-c *plane of V_6O_{13}. Contour intervals plotted at 0.05 e/Å³; negative regions are represented by solid lines; positive regions are represented by dashed lines; zero level removed.*

https://doi.org/10.1557/mrs2000.64 Published online by Cambridge University Press